

Use of annealed low-temperature grown GaAs as a selective photoetch-stop layer

E. H. Chen, D. T. McInturff, T. P. Chin, M. R. Melloch, and J. M. Woodall^{a)}

School of Electrical and Computer Engineering and NSF-MRSE Center for Technology Enabling Heterostructure Materials, Purdue University, West Lafayette, Indiana 47907-1285

(Received 15 December 1995; accepted for publication 17 January 1996)

We demonstrate annealed low-temperature grown (LTG) GaAs to be a highly effective etch-stop layer while photoetching *n*-type normal-growth-temperature GaAs. During this process, the etch rate is controlled by the transport of photogenerated carriers to the semiconductor/electrolyte interface. Because of the very short minority carrier lifetime in LTG-GaAs, only a very small portion of photogenerated carriers can reach the semiconductor surface to complete the electrolytic decomposition reaction. Therefore, the etch rate of LTG-GaAs is reduced considerably. In our studies, the etch rate selectivity can be as high as 800. Furthermore, we demonstrate that doping concentration, presence of an ohmic contact, photon energy, and *pH* value of the etching solution can be used to control the etch rate of *n*-GaAs during the photoetching process. © 1996 American Institute of Physics. [S0003-6951(96)03112-3]

In both electronic and optoelectronic devices, GaAs is one of the most commonly used semiconductor materials. Selective etching of GaAs layers is often required in device processing. Several different techniques have been reported including: selective reactive ion etching (dry etching),^{1,2} selective wet etching,^{3,4} and bandgap-selective photoetching.^{5,6} However, all of these techniques require a different material, Al_xGa_{1-x}As, as the etch stop layer, and each of them exhibits disadvantages. The process of dry etching, for example, is relatively complicated and damage produced by energetic ion bombardment may cause degradation of device performance.⁷ The selectivity of GaAs on Al_xGa_{1-x}As in wet etching is relatively low unless one uses a high mole fraction of aluminum. But Al_xGa_{1-x}As with high Al composition is strongly susceptible to the formation of Al_xO_y, which can degrade the long-term device stability.³ As for bandgap-selective photoetching, the photon energy of the light source has to be carefully selected between the bandgap energy of GaAs and Al_xGa_{1-x}As. Therefore, its application is also limited. We show in the present letter that annealed low-temperature grown (LTG) GaAs (referred to as GaAs:As) can be used as an effective photoetch-stop layer with relatively simple procedures. In addition, the etch rate can be optimized by varying different parameters such as doping level, use of an ohmic contact, wavelength of the light source, and *pH* value of the electrolyte.

Figure 1 shows the schematic band diagrams for an *n*-type semiconductor/electrolyte interface under different conditions. The simplest photoetching mechanism can be illustrated as Fig. 1(a) when the system is under thermal equilibrium. A Schottky barrier is formed at the liquid–solid interface. The Schottky barrier height is determined by the work function difference between the semiconductor (Φ_s) and the electrolyte (Φ_E). Because Φ_E is a function of *pH* value,⁸

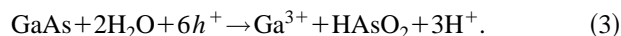
$$\Phi_E = 4.25 + 0.059 \times \text{pH} \text{ (eV)}. \quad (1)$$

We can modulate the barrier height and, therefore, the depletion width by adjusting the *pH* value of the electrolytic solution. When above-bandgap photons are absorbed at the surface of the semiconductor, electron-hole pairs are created. In the case of an *n*-type semiconductor, the built-in electric field of the surface space-charge region will transport holes to the semiconductor/electrolyte interface and electrons to the bulk. Because of the existence of holes at the liquid–solid interface, GaAs will be oxidized via the following reactions.

at high *pH*



at low *pH*



These oxides are then chemically dissolved into the solution.^{9,10}

It is well known that the minority carrier lifetime of GaAs:As material is only about several picoseconds,^{11,12} which is several orders of magnitude smaller than that of normal GaAs material. Because of their short lifetime, nearly all of the photogenerated holes in a GaAs:As layer will recombine before reaching the semiconductor/electrolyte interface to react with surface GaAs atoms. As a consequence of this, the photoetching reaction will be greatly reduced in GaAs:As material, and thus a high etch selectivity should result between GaAs and GaAs:As.

The films used in this study were grown in a Varian Gen II molecular beam epitaxy (MBE) system with As₂ for the group V source and elemental Ga for the group III source. The beam equivalent pressure ratio of As₂ to Ga was ≈ 10 . Each structure consists of a 1500 Å undoped GaAs layer grown at 250 °C followed by a 3 μm GaAs top layer grown at 600 °C with two different Si doping levels of $2 \times 10^{16} \text{ cm}^{-3}$ and $2 \times 10^{18} \text{ cm}^{-3}$. Because of the 3 μm GaAs top layer, the LTG-GaAs was in fact annealed at 600 °C for about 3 h *in situ*.

Samples from each growth were placed inside a culture dish, filled with etching solution, and light was directed onto the top GaAs surface. Two different aqueous solutions were

^{a)}Electronic mail: woodall@ecn.purdue.edu

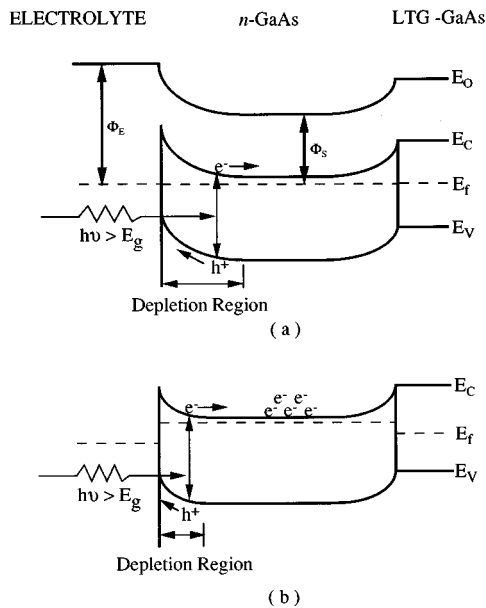


FIG. 1. Schematic energy band diagrams of an *n*-type semiconductor/electrolyte interface under (a) thermal equilibrium and (b) high power illumination.

examined: high *pH* basic solution, 1M KOH, and low *pH* acid solution, 0.5M H₂SO₄. The specific reagent compositions were 97% H₂SO₄ by volume, and 85% KOH by weight. Two light sources, a 4.5 mW 633 nm He/Ne laser and a 7.5 mW 442 nm He/Cd laser, were used. For the measurements, a stylus profilometer with the resolution about 50 Å was used to determine the depth of the etched surface.

Curves I in Fig. 2(a) show the etch depth for *n*-type GaAs in KOH solution as a function of etch time for the He/Ne red laser (633 nm). A typical curve is characterized by an initial linear increase followed by a saturation plateau at 3 μm depth, which is exactly the thickness of the top GaAs layer. This demonstrates that the etching reaction was effectively stopped at the GaAs/GaAs:As interface. The selectivity, which is defined as the ratio of the etch rates of GaAs to GaAs:As, can be determined by comparing the slopes between the plateau and initial linear regions. The selectivity was measured to be at least 600 and is 4 times better than obtained using Al_{0.3}Ga_{0.7}As as the etch-stop layer in regular selective wet etching. However, the quantum efficiency (QE) which is defined as

$$QE = \frac{\text{Removed GaAs Molecules}}{\text{Incident Photons}} \times 6 \quad (4)$$

is only about 1.6% without correcting for reflection losses. Furthermore, curves I also show that for different doping concentrations, $2 \times 10^{16} \text{ cm}^{-3}$ and $2 \times 10^{18} \text{ cm}^{-3}$, the etch rates on GaAs material show no significant difference. These results are not consistent with the photoetching mechanism mentioned above; the sample with the lower doping level is expected to have a higher reaction rate because its wider surface depletion region enables more photogenerated holes to be transported to the surface for the oxidation reaction.

The observed low quantum efficiency and lack of any doping dependency can be attributed to the self-biased con-

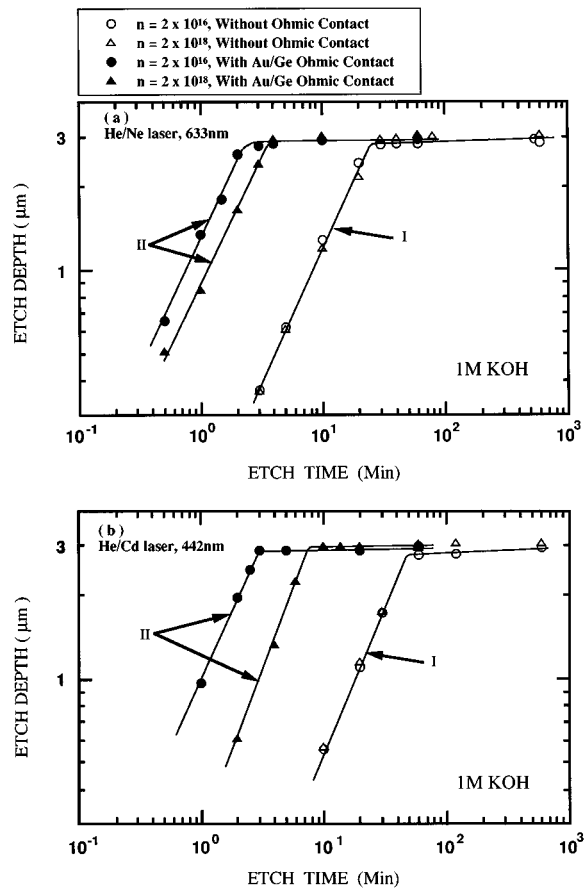


FIG. 2. Etch depth for *n*-type GaAs as a function of etch time. Results are compared for samples with (curves II) and without (curves I) Au/Ge/Ni ohmic contact, and for different light sources: (a) He/Ne red laser, 633 nm (b) He/Cd blue laser, 442 nm.

dition of the semiconductor/electrolyte interface. A more precise understanding of the electrochemical circuit can be visualized by viewing the energy band diagram of this system in Fig. 1(b) under high power illumination. For every hole that drifts to the surface and reacts, one electron is left behind. Because of the electron barriers at both the top electrolyte/*n*-GaAs and the bottom *n*-GaAs/GaAs:As interfaces of our structure, these majority carriers keep accumulating within this *n*-type GaAs layer until the total electron current is balanced with the total hole current since the etch is electroless. Therefore, under high power illumination, the background doping concentration does not play any significant role because of this electron accumulation. Furthermore, the electrolyte/GaAs interface is under a forward-bias condition and therefore the flow of minority carriers to the interface is greatly reduced. Consequently, the etching reaction is also greatly reduced. In order to increase its quantum efficiency, the system needs to be maintained as close to its equilibrium state as possible by draining those accumulated electrons into the solution. Since for *n*-GaAs electrons are able to travel a long distance through the crystal, putting an ohmic contact on the dark surface will assist the electrons flow into solution and therefore increase the etch rate. To demonstrate this, we deposited alloyed Au/Ge/Ni ohmic contacts on top of the same structure described previously. A hole in the contact was left to allow the etching reaction to

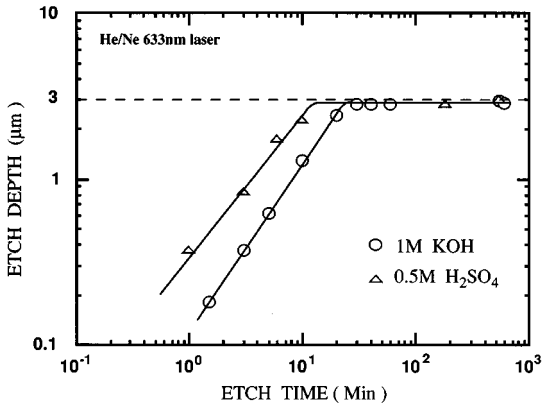


FIG. 3. Etch depth of GaAs ($n=2 \times 10^{16} \text{ cm}^{-3}$) as a function of etch time in two different etching solutions, high pH 1M KOH (○) and low pH 0.5M H_2SO_4 (△) by using He/Ne red laser.

take place. In addition, a palladium wire was connected electrically with silver paste to the metal contact and subsequently cemented and partly covered with black wax. The Pd was chosen because of its inert property for the study of charged carrier transport in electrochemistry.

The same experiments were performed again in 1 M KOH solution and the results are shown in curves II in Fig. 2(a). Clearly, the etching efficiency has been dramatically increased to about 10 and 6 times for the $2 \times 10^{16} \text{ cm}^{-3}$ and $2 \times 10^{18} \text{ cm}^{-3}$ doped samples, respectively. The etch rate difference between the different doping levels is as expected; the lower the doping concentration, the higher the etch rate.

We performed similar experiments to those described above except a shorter wavelength 442 nm He/Cd blue laser was used instead of the 633 nm He/Ne red laser. The results are presented in Fig. 2(b) and they are qualitatively similar to those shown in Fig. 2(a) for the longer wavelength red laser. One of the noticeable differences using the short wavelength He/Cd laser was that we were able to achieve a higher quantum efficiency, at least a 150% increase, than with the long wavelength He/Ne red laser. Note that because of the higher energy per photon and larger laser beam size of the He/Cd blue laser, the total volumetric hole production per unit incident laser intensity is smaller than that of the He/Ne red laser. Thus, even though the etch rates showed in Fig. 2(b) are slower than those shown in Fig. 2(a), the QE is actually higher. We also observed stronger doping dependency in this case of using the short wavelength laser. The higher QE and stronger doping dependency are due to the fact that the shorter wavelength photons are absorbed closer to the surface and consequently, (i) a higher fraction of photogenerated holes are created inside the space charge region and subsequently driven to the surface by the electric field prior to recombination, and (ii) the etch is also much more sensitive to the variation of surface depletion width because of the

exponential decay of incident photon flux. After ohmic contact formation, the quantum efficiency for the $n=2 \times 10^{16} \text{ cm}^{-3}$ samples has been increased from 2.4% to 40% without correcting for reflection losses.

Figure 3 shows the etch depth for GaAs ($n=2 \times 10^{16} \text{ cm}^{-3}$) without an ohmic contact on the surface for two different etching solutions, 0.5M H_2SO_4 and 1M KOH, as a function of etch time with the He/Ne red laser (633 nm). The etch rate in low pH H_2SO_4 acid solution was about twice as fast as the etch rate in the high pH KOH basic solution. We attribute this increase to the decrease in the Schottky barrier height because from Eq. (2) we know that the low pH electrolyte has a lower work function. Hence, the potential barrier is lower in the acid solution and electrons more readily flow into the solution. Again, the selectivity was determined by comparing the slopes between the saturation and initial linear regions of the curves in Fig. 3. The selectivity is as high as 800 in the 0.5M H_2SO_4 solution.

In summary, we have developed a new technique for selective etching of the GaAs material system by using GaAs:As as an etch-stop layer in a photoetching process. This technique gives high selectivity, and yet the processing is not complicated. The etch rate on *n*-GaAs as a function of doping level, photon energy, and pH value of electrolyte has also been investigated. High etching efficiency can be achieved by using (i) high energy photons, (ii) samples with an ohmic contact, (iii) low doping concentration, and (iv) a low pH acid electrolyte. Finally, this idea can be extended to the AlGaAs:As material system, providing an additional degree of freedom for device design.

This work was supported by the Materials Research Science and Engineering Center from the National Science Foundation Grant No. DMR-9400415 and the Air Force Office of Scientific Research Grant No. F49620-93-1-0031.

- ¹M. Walther, G. Trankle, T. Rohr, and G. Weimann, *J. Appl. Phys.* **72**, 2069 (1992).
- ²M. Tong, D. G. Balleger, A. Ketterson, E. J. Roan, K. Y. Cheng, and I. Adesida, *J. Electron. Mater.* **22**, 9 (1992).
- ³G. C. DeSalvo, W. F. Tseng, and J. Comas, *J. Electrochem. Soc.* **139**, 831 (1992).
- ⁴C. Juang, K. J. Kuhn, and R. B. Darling, *J. Vac. Sci. Technol. B* **8**, 1122 (1990).
- ⁵R. Khare, D. B. Young, and E. L. Hu, *J. Electrochem. Soc.* **140**, L117 (1993).
- ⁶R. T. Brown, J. F. Black, R. N. Sacks, G. G. Peterson, and F. J. Leonberger, *Mater. Res. Soc. Symp. Proc.* **75**, 411 (1987).
- ⁷S. Salimian, C. Yuen, C. Shin, and C. B. Cooper, *J. Vac. Sci. Technol. B* **9**, 114 (1991).
- ⁸H. O. Finkia, *Semiconductor Electrodes* (Elsevier Science, The Netherlands, 1988).
- ⁹H. Gerische, *J. Vac. Sci. Technol.* **15**, 1442 (1978).
- ¹⁰J. Van De Ven and H. J. P. Nabben, *J. Electrochem. Soc.* **137**, 1603 (1990).
- ¹¹E. S. Harmon, M. R. Melloch, and J. M. Woodall, *Appl. Phys. Lett.* **63**, 2248 (1993).
- ¹²M. R. Melloch, J. M. Woodall, E. S. Harmon, N. Otsuka, F. H. Pollak, D. D. Nolte, R. M. Feenstra, and M. A. Lutz, *Annu. Rev. Mater. Sci.* **25**, 547 (1995).